Автоматизовані системи управління та прилади автоматики. 2026. № 2 (189) *ISSN 3083-7715 (online)*
Management Information System and Devices. 2026. No. 2 (189) *ISSN 3083-7650 (0135-1710) (print)*

UDC 004.8:519.876 DOI: https://doi.org/10.30837/0135-1710.2026.189.309

Stanislav Pohorielov, Yaroslav Balaba, Maksym Tatariaiants, Yevhen Berkunskyi, Alona Pavlenko

A SYSTEMATIC SENSITIVITY STUDY OF PHYSICS-INFORMED NEURAL NETWORKS FOR EPIDEMIC TIME SERIES

This paper presents a systematic sensitivity analysis of Physics-Informed Neural Networks (PINN) applied to epidemic time-series modeling. **The objective** of the study is carrying out of a systematic analysis of the sensitivity of PINN models on real epidemic time series and identification of the key factors governing the quality of epidemic-wave dynamics reconstruction. **Tasks:** assessment of the impact of sliding-window length, the set of covariates, regularization parameters, and random initialization on PINN quality; benchmarking PINN against a classical baseline model without physical constraints. **Methods:** an extensive series of experiments across three countries with varying sliding-window length, window stride, fractional derivative order α, stochastic stability, and sets of covariates; statistical analysis using the Wilcoxon test, OLS with HC3 correction, PCA, and Lasso regularization. **Results:** PINN almost consistently outperforms the baseline in reproducing epidemic time series, yielding higher R^2 values and lower RMSE/MAE across all countries. A 14-day sliding window provides the optimal balance between model adaptability and stability, whereas extending the window length to 21 days leads to over-smoothing of the dynamics and loss of local sensitivity. The experimental results indicate that the effect of covariates does not exhibit a universally positive impact. In certain configurations and countries, additional predictors improve model quality, while in others they introduce noise owing to multicollinearity and poor data quality. The stability analysis confirms that PINN is largely insensitive to random initialization and regularization hyperparameters. The findings provide a clear characterization of PINN behavior in epidemiological modeling tasks and yield practical recommendations for parameter selection that ensure model reliability and reproducibility. **Conclusions:** PINN is a more effective alternative to classical models for epidemic modeling; a 14-day sliding window is optimal; the effect of covariates is unstable and country-dependent.

Key words: physics-informed neural networks (PINN); epidemic time series, sensitivity analysis; sliding window; covariates; model stability; machine learning; epidemiological modeling.

1. Introduction

Mathematical modeling of epidemic processes remains one of the key tools for analyzing the dynamics of infectious diseases and supporting decision-making in the field of public health [1]. During the COVID-19 pandemic, SIR and SEIR models were actively used to analyze the impact of anti-epidemic measures and to explore possible scenarios of tightening or relaxing control measures. In particular, it was shown that the use of Caputo fractional derivatives allows for the natural incorporation of memory and inertia effects [1, 2], while the application of neural networks enables the adaptive reproduction of the temporal variability of infection and recovery parameters [3–5]. These results formed the basis for the further development of models capable of combining the interpretability of analytical equations with the flexibility of data-driven methods [6–8].

Literature Review

The classical SIR models proposed in [1] became the foundation of mathematical modeling of epidemics. The authors of [2] revisited classical SIR modeling in the context of the COVID-19 pandemic. In [3], the SIR model is applied to forecast the spread of COVID-19 in Ukraine.

A separate line of research is related to the application of fractional derivatives in epidemic models. The authors of [9] proposed a fractional SIR model for COVID-19. In [10], the problem of optimal control based on a fractional SIR model with a Caputo derivative was investigated, and in [11], the order of the fractional derivative was optimized to improve modeling accuracy.

Physics-informed neural networks (PINNs) as an approach to solving differential equations using neural networks were systematized in [6, 7]. This approach combines the flexibility of machine learning with physical constraints, ensuring the interpretability and accuracy of models.

A comprehensive review of the current state of PINN methodology, including architectural solutions, optimization methods, and open problems, is presented in [12]. Wang et al. [13] investigated the causes of PINN training instability from the perspective of neural tangent kernels and proposed adaptive weights to balance the components of the loss function. Kharazmi et al. [14] applied PINN to the parameter identification of fractional epidemic models, demonstrating the advantages of

ISSN 3083-7715 (online) Автоматизовані системи управління та прилади автоматики. 2026. № 2 (189)
ISSN 3083-7650 (0135-1710) (print) Management Information System and Devices. 2026. No. 2 (189)

a physics-informed approach for forecasting the dynamics of COVID-19. The issue of self-adaptive PINN training is discussed in [15], and a review of PINN applications in continuum mechanics is provided in [16].

An evaluation of ensemble forecasts of COVID-19 mortality, highlighting the importance of validating models on real data, is presented in [17]. Theoretical guarantees of PINN generalizability for inverse problems are investigated in [18].

However, most previous studies have focused either on synthetic data or on reconstructing hidden trajectories within the framework of fractional models $S(t)$, $I(t)$, $R(t)$ within the framework of fractional models. Much less attention has been paid to the practical aspects of applying Physics-Informed Neural Networks (PINNs) to real-world epidemic time series, particularly issues of stability, parameter sensitivity, and the influence of input data structure. In real-world conditions, models face a number of challenges: data noise, uneven sampling, changes in behavioral and social factors, multicollinearity of additional variables, as well as the dependence of results on the choice of the interval length over which the model is trained and the method of its progression along the time series. Analysis of these factors complicates the practical application of PINN in epidemiological modeling tasks [6–8]. The absence of such systematic checks significantly complicates the practical application of PINN.

The aim of this work is to conduct a systematic sensitivity analysis of PINN models on real epidemic time series and to identify the key factors influencing the quality of the reproduction of epidemic wave dynamics.

The article investigates the influence of three key groups of factors:

1) structural modeling parameters, specifically the length of the data interval used for local model training and the frequency of its shifting;

2) information content, i.e., the set of additional variables (covariates) that may influence the dynamics;

3) stochastic and regularization aspects that determine the reproducibility of results and the model's robustness to variations in initial conditions.

A large-scale series of experiments was conducted for three countries, which allowed us to assess the stability of the PINN, compare it with a classical model without physical constraints, and form a generalized picture of the model's behavior under various conditions.

Particular attention was paid to how changes in the length of the training interval, the frequency of its shift, and the set of covariates affect the accuracy of reproducing epidemic dynamics, as well as to the extent to which the results remain stable when stochastic factors change.

Thus, this work continues the logical line of the authors' previous research, moving from the theoretical analysis of fractional models and hybrid approaches to the practical evaluation of their effectiveness on real data. The results obtained allow us to formulate recommendations regarding the selection of PINN model parameters that ensure their reliability, robustness, and interpretability in epidemiological modeling tasks.

2. Methodology

This section describes the data structure, the preprocessing procedure, the principles for forming training samples, the model structure, optimization parameters, the approach to sensitivity analysis, and the statistical processing of results. Particular attention is paid to ensuring the reproducibility of experiments and the validity of comparisons between the classical model and physically informed neural networks (PINN).

2.1. Data and Rationale for Country Selection

For our study, we used open daily incidence data published by the **Our World in Data** project (University of Oxford) [19]. From this dataset, we selected three countries: Germany, Italy, and Ukraine. This selection is formally justified based on three factors.

First, these countries have different population sizes, which allows us to assess the stability of the models under various demographic conditions. Germany represents a large European population, Italy a medium-sized one, and Ukraine a medium-sized one with a different age and mobility structure.

Second, the countries demonstrate varying quality and completeness of epidemic data. Germany's data are among the most stable and systematic in Europe; Italy is characterized by high variability at the onset of waves; Ukraine exhibits significant noise and uneven testing. This allows us to assess how robust the PINN models are to varying data quality.

Third, these countries have different covariate profiles, particularly regarding vaccination, testing, and the strictness index of restrictions. This allows us to

Автоматизовані системи управління та прилади автоматики. 2026. № 2 (189) *ISSN 3083-7715 (online)*
Management Information System and Devices. 2026. No. 2 (189) *ISSN 3083-7650 (0135-1710) (print)*

investigate whether the effect of covariates is universal or depends on the country.

For each country, we selected one epidemic wave covering the period from the autumn surge to the spring decline. The main observed variable is the daily incidence rate per 100,000 population:

$$Y_{\text{data}}(t) = \frac{new\_case\_smoothed(t)}{N} \cdot 10000 \qquad (2.1)$$

where $new\_case\_smoothed(t)$ is the 7-day smoothed number of new cases, and N is the country's population.

The data is sorted by date and divided into training (60%) and test (40%) sets.

2.2. Formal Formulation of the Problem

All models operate within the framework of a discrete SIR structure [1]. Let:

$S(t)$ – the number of susceptible individuals at time t;

$I(t)$ – the number of infected individuals;

$R(t)$ – the number of removed (recovered or deceased);

$\tilde{N} = 100000$ – effective population (scaling for stability).

Then the following holds:

$$S(t) + I(t) + R(t) = \tilde{N}. \qquad (2.2)$$

In the classical SIR model, the dynamics are given by:

$$\begin{aligned} S(t+1) &= S(t) - \beta(t) S(t) I(t), \\ I(t+1) &= I(t) + \beta(t) S(t) I(t) - \gamma(t) I(t), \\ R(t+1) &= R(t) + \gamma(t) I(t) \end{aligned} \qquad (2.3)$$

where $\beta(t)$ is the transmission coefficient, and $\gamma(t)$ is the withdrawal coefficient.

In this study, $\beta(t)$ and $\gamma(t)$ are assumed to be constant within each sliding window but may vary between windows.

The model incidence is defined as:

$$Y_{\text{model}}(t) = \beta(t) S(t) I(t). \qquad (2.4)$$

The study employs the FSIR model, which uses the Caputo fractional derivative of order $\alpha \in (0,1]$:

$${}^{C}D_t^{\alpha} f(t) = \frac{1}{\Gamma(1-\alpha)} \int_0^t (t-\tau)^{-\alpha} f'(\tau) d\tau, \qquad (2.5)$$

where $\Gamma(\cdot)$ is the gamma function, which extends the concept of the factorial to real arguments, and $f'(\tau)$ is the ordinary derivative of the function f with respect to time [20, 21].

This allows us to naturally account for the memory and inertia effects of the epidemic process. The fractional derivative enables smooth interpolation between classical Markov dynamics $(\alpha = 1)$ and processes with long memory $(\alpha < 1)$ [9–11, 22]. A discrete $L1$ approximation was used to approximate the fractional derivative. Let $x_n = x(t_n)$ be the values of the scalar sequence at the nodes $t_n = n\Delta t$. According to the $L1$ scheme, the Caputo fractional derivative of order α is approximated as:

$${}^{C}D_t^{\alpha} x(t_n) \approx \sum_{k=0}^{n-1} \alpha_{n-k} \left(x(t_{k+1}) - x(t_k) \right), \qquad (2.6)$$

where the weights a_m are specified analytically and take the form:

$$a_m = (m+1)^{1-\alpha} - m^{1-\alpha}, \; m \geq 0. \qquad (2.7)$$

For practical implementation with a fixed window of length L, we compute the weights $a^0, \ldots, a_{L-1}$ and for each step $n = 1, \ldots, L-1$ we use

$$D_n = \sum_{m=0}^{n-1} a_m \Delta x_{n-1-m}, \; \Delta x = x_{j+1} - x_j. \qquad (2.8)$$

A naive implementation of computing all D_n has asymptotic complexity of $O(L^2)$ for a single window. Optimized tensor approaches reduce the constants, but the order remains quadratic. For $n = 0$, we assume $D^0 = 0$.

2.3. Hyperparameters and Covariates

For local learning, a sliding window of length L is used. Let t_k be the start of the k-th window. Then the window covers $t \in \{t_k, t_k + 1, t_k + L - 1\}$. In this work, we considered two window lengths: $L \in \{14, 21\}$. We denote the shift step between windows by s. The default value is $s = 7$, and for sensitivity analysis, we additionally considered $s = 3$ and $s = 10$.

All model parameters $\beta(t)$ and $\gamma(t)$ are considered constant within the window $[t_k, t_k + L - 1]$.

Let $X(t) \in R^m$ be the vector of covariates at time t. The following variables (covariates) were used in the experiments: vaccination and its lags, the restriction stringency index, testing rates, the proportion of positive tests, and the number of new tests.

2.4. Models

Baseline is a classic machine learning model that approximates the relationship:

$$Y_{\text{model}}(t) = f_{\theta}(X(t)), \qquad (2.9)$$

where f_{θ} is a multilayer perceptron.

ISSN 3083-7715 (online) Автоматизовані системи управління та прилади автоматики. 2026. № 2 (189)
ISSN 3083-7650 (0135-1710) (print) Management Information System and Devices. 2026. No. 2 (189)

The model imposes no physical constraints and serves as a baseline for evaluating the advantages of PINN. The baseline model is implemented as a lightweight MLP head (BetaGammaHead class) with three hidden layers of 64 neurons each and tangent-hyperbolic activations; the output consists of two linear components, which are converted via softplus into non-negative sequences: $\beta(t)$ and $\gamma(t)$. The head's input size corresponds to the number of predictors in the window (normalized time and covariates). For each sliding window, the head is initialized with a deterministic random seed (the seed depends on the window number), after which it is optimized separately for the baseline version, minimizing only the MSE between the forecast Y_{hat} (computed via FSIR-forward using the obtained $\beta(t)$, $\gamma(t)$) and the observations. Training is performed using the Adam optimizer $\left(lr \approx 2 \cdot 10^{-3}\right)$ for 400 epochs, with the best snapshot selected based on the minimum loss within the window. This approach ensures that the baseline and PINN start with the same initial weights for a fair comparison.

The physics-informed neural network combines trajectory approximation S, I, R with the execution of discretized FSIR equations [6].

Let $\tau \in [0,1]$ be the normalized time within the window. PINN approximates:

$$\left(S(\tau), I(\tau), R(\tau)\right) = f_\theta(\tau), \tag{2.10}$$

where f_θ is an MLP with three hidden layers.

In physically informed neural networks that approximate the trajectories $S(t)$, $I(t)$, $R(t)$, it is important to ensure that the basic structural properties of the SIR model are satisfied: non-negativity of components and approximate constancy of the total population. Standard neural networks do not guarantee these constraints, as their outputs can take on arbitrary real values. The use of hard activations (e.g., ReLU) leads to gradient issues and optimization instability, which is critical in PINNs, where physical equations are directly incorporated into the loss function [6, 7].

For this reason, the model employs softplus normalization, which ensures a smooth and guaranteed non-negative transformation of the network outputs and approximate constancy of the $(S+I+R)$:

$$\text{swoftplus}(x) = \ln\left(1+e^x\right) > 0. \tag{2.11}$$

Based on these three values u, v, w, a normalized distribution is formed:

$$\begin{aligned} S &= \tilde{N}\frac{u}{u+v+w}, \\ I &= \tilde{N}\frac{v}{u+v+w}, \\ R &= \tilde{N}\frac{w}{u+v+w}, \end{aligned} \tag{2.12}$$

which guarantees $S, I, R \geq 0$ and $\left(S+I+R \approx \tilde{N}\right)$.

Softplus is infinitely differentiable, has no "dead" zones, and ensures stable gradients. PINN minimizes the deviation between the network output and the right-hand sides of the SIR equations:

$$\delta^2 = \left|(S,I,R) - \left(S^{\text{FSIR}}, I^{\text{FSIR}}, R^{\text{FSIR}}\right)\right|^2. \tag{2.13}$$

Loss function:

$$L = L_{\text{data}} + \lambda_{\text{phys}} L_{\text{phys}} + \lambda_{\text{reg}} L_{\text{reg}}, \tag{2.14}$$

where the first term accounts for data fit, the second for satisfying the physical equations, and the third for regularization.

2.5. Training, optimization, metrics, and sensitivity analysis

Training is performed separately on each window. The parameters of the next window are initialized with the values from the previous one (warm start), which ensures smooth trajectories.

The Adam optimizer was chosen, which has already become the standard in all PINN studies. Adam automatically scales gradients for each parameter, which is critically important when the loss function contains both a physical term and a data term, as well as when the neural network weights, the parameters $\beta(t)$ and $\gamma(t)$, and the physical and data losses differ in magnitude by several orders of magnitude [23]. Adam's adaptability ensures robustness against noisy and poorly scaled gradients, which are characteristic of models with physical constraints. Furthermore, Adam performs well in "warm start" mode, where the parameters of each subsequent epoch are initialized with the values from the previous one, which promotes smooth trajectories and accelerates convergence.

Data for each country are first truncated to the selected wave and sorted by date; the primary unit of analysis is daily incidence per 100,000 population. For local model training, a sliding window of length L ($L \in \{14, 21\}$ in experiments) is used with a stride step

Автоматизовані системи управління та прилади автоматики. 2026. № 2 (189) *ISSN 3083-7715 (online)*
Management Information System and Devices. 2026. No. 2 (189) *ISSN 3083-7650 (0135-1710) (print)*

(base case stride = 7, additional ablations 3 and 10). For each window, the baseline and PINN are trained separately with the same initialization (a deterministic seed dependent on the window number), after which forecasts from all windows covering a given time point are aggregated by averaging (taking into account the number of overlaps). After aggregation across the entire time series, a global split into training and test sets is formed: the first 60% of observations are used to evaluate training metrics, the remaining 40% for the final evaluation (train/test = 0.6/0.4). For each window, the best model snapshot is saved based on the minimum MSE loss in that window. It is these best local forecasts that are aggregated to construct the final Y_{model} and subsequently calculate $RMSE$ / MAE / R^2.

The hyperparameters were determined by combining preliminary tests and targeted ablation studies (sensitivity analysis) rather than a single large-scale automated search. The following values were selected as working baseline values: learning rate for both models $lr \approx 2 \cdot 10^{-3}$, number of epochs per window for the baseline – 400, for PINN – 500; regularization term weights $\lambda_{\text{phys}} = 0.1$, $\lambda_{\text{L\_reg}} = 0.01$, $\lambda_{\text{smooth\_b}} = 10^{-3}$; order of the fractional derivative $\alpha \in \{0.7, 0.9, 1.0\}$. A series of controlled experiments was conducted in which key parameters were varied sequentially (window length, stride, α, covariate sets, λ values, and seed), and performance was evaluated using aggregated test metrics (specifically, the average RMSE across all windows and seeds). For PINN, a "warmup" is applied – the physical term $\lambda_{\text{phys}} L_{\text{phys}}$ begins to take full effect after 40% of the epochs, which reduces the risk of the physical penalty dominating the data fitting too early. The criterion for selecting the configuration is the minimization of the test $RMSE$ (supplemented, if necessary, by a check of result stability across different seeds and countries). The final parameter values were chosen as a compromise between forecast quality and stability/reproducibility across all three countries.

For each model, the following are calculated: $RMSE$, MAE, and R^2 on the training and test sets. Stability with respect to changes in random initialization and regularization parameters is evaluated separately.

The sensitivity analysis covers three groups of factors:

1) structural parameters (window length, shift frequency),

2) informational parameters (set of covariates),

3) stochastic parameters (initialization, regularization).

2.6. Statistical Analysis

Statistical hypothesis testing and statistical analysis of the obtained results include data preparation, test selection, correction for multiple comparisons, estimation of effect size, construction of confidence intervals, and additional models for generalizing conclusions.

For each group of differences (RMSE PINN minus Baseline), we test the normality of the distribution of differences using the Shapiro–Wilk test. If the Shapiro–Wilk test does not reject normality, we apply the paired t-test. If normality is rejected or there is suspicion of outliers, we apply the nonparametric Wilcoxon signed-rank test. To compare the effect of the sliding window length $(L14)$ versus $(L21)$, we use paired tests on corresponding pairs when such pairs are available; if the pairs are aggregated, we apply a *one-sample* test for differences or a nonparametric equivalent.

Next, a correction for multiple comparisons is applied [24]. To control the proportion of false-positive results, the Benjamini-Hochberg FDR is applied. To assess the effect size in paired comparisons, the paired Cohen's d is provided along with its interpretation. Statistical significance is accompanied by an effect size estimate and confidence intervals.

Due to possible heteroscedasticity of residuals in regression models, standard errors may be underestimated. To mitigate this effect, the HC3 method is used, which provides a more conservative correction, especially with small samples or in the presence of outliers [25, 26]. In all regression estimates of coefficients and when constructing mixed models, standard errors and confidence intervals are reported with HC3 correction. The tables indicate that standard errors are HC3-corrected.

For a generalized conclusion, this study constructed a mixed linear model with fixed effects for model type and window length and a random effect for country [27]. Such a model allows for accounting for the correlation of observations within a country and for estimating the overall impact of the transition from Baseline to PINN. The paper presents estimates of fixed effects, standard errors of HC3, and an interpretation of the coefficients in terms of changes in RMSE.

To check for multicollinearity among predictors, we calculated the variance inflation factor (VIF) using

ISSN 3083-7715 (online) Автоматизовані системи управління та прилади автоматики. 2026. № 2 (189)
ISSN 3083-7650 (0135-1710) (print) Management Information System and Devices. 2026. No. 2 (189)

the standard formula [28–30]. All values were VIF < 3.6, indicating the absence of serious multicollinearity.

All calculations were performed using Python version 3.13.5 (packages: pandas, scipy, numpy, statsmodels, seaborn, matplotlib, sklearn) [31, 32].

The main limitations of the statistical analysis are small sample sizes (interpretation should be cautious in groups with small n); the absence of complete pairs by seed (some configurations do not have complete pairs by seed, so some comparisons were performed in an aggregated manner); sensitivity to test selection (some results depend on the choice of a paired or nonparametric test, and this is accounted for in the report and in the correction for multiple comparisons).

3. Results

This section presents the results of a systematic comparison of the physically-informed neural network (PINN) model with a baseline machine learning model, as well as an analysis of the PINN's sensitivity to key structural, informational, and stochastic factors. The focus is on a practical assessment of the model's stability, generalizability, and factor-dependent quality on real-world epidemic data.

The analysis covers 118 experimental configurations that differ in sliding window length, set of covariates, regularization parameters, order of the fractional derivative (α), window shift step, and random initialization.

The section is structured to sequentially answer three key questions:

To what extent does the PINN model consistently outperform the baseline model? This question is addressed in subsection 3.1, which presents aggregated results for all countries and configurations.

Which structural parameters (window length, stride, fractional order) have the greatest impact on model quality? This is the subject of Section 3.2, which analyzes the role of the sliding window and hyperparameters.

Do the covariates (vaccination, testing, severity index, etc.) have a statistically significant additional effect? This question is addressed in Section 3.3, which presents the results of nonparametric tests, robust regression, decomposition (R^2), PCA, and the regularized Lasso model.

Particular attention is paid to the fact that, despite theoretical expectations, none of the covariates demonstrated a consistent statistically significant effect on PINN returns, and the effect of covariates varies by country. In some configurations, additional variables ( ) yield a slight improvement, while in others they worsen performance due to noise or multicollinearity. This result warrants separate discussion, as it contradicts the intuitive assumption that adding information on vaccination, testing, or the strictness index should improve model quality.

3.1. General Comparison of PINN and the Baseline Model

The first stage of the analysis is a comparison of the physically informed neural network (PINN) with the baseline machine learning model (Baseline), which contains no physical constraints and serves as a reference point for evaluating the effectiveness of PINN. For each of the 118 experimental configurations, the root mean square error (*RMSE*), *mean absolute error* (*MAE*), and R^2 were calculated on the test dataset, along with the performance gain of PINN over the baseline model. The difference between the models' errors was used as the comparison metric:

$$\Lambda = RMSE_{\text{baseline}} - RMSE_{\text{PINN}} . \qquad (3.1)$$

where the $\Delta > 0$ indicates the advantage of PINN. This metric allows us to quantitatively assess the gain provided by the model's physical structure, i.e., to what extent the physical constraints and structural properties of PINN improve the model's ability to reproduce epidemic dynamics.

In all configurations, PINN outperforms the standard baseline model and does so consistently across all three countries. The average gain is $\left(\bar{\Delta} = 1.3301\right)$, with a 95% confidence interval of [1.1920; 1.4682]. The Wilcoxon nonparametric test for paired samples yields $p \ll 0.001$, which corresponds to a very large effect on the Cohen scale $(d = 2.12)$. This indicates a systematic advantage of PINN that is not an artifact of specific configurations or random initialization.

Figure 3.1 shows the distributions of *the* test *RMSE* for Baseline and PINN separately by country. Violin plots have been constructed for each country, showing the shape of the distribution, median values, and spread. It is evident that for all countries, PINN demonstrates lower median *RMSE* values

Автоматизовані системи управління та прилади автоматики. 2026. № 2 (189) *ISSN 3083-7715 (online)*
Management Information System and Devices. 2026. No. 2 (189) *ISSN 3083-7650 (0135-1710) (print)*

and a smaller spread, indicating higher accuracy and model stability. The greatest improvement is observed in Italy, where the epidemic wave has a complex shape with pronounced asymmetry. In Ukraine, the improvement is moderate but stable, while in Germany it is the smallest, although PINN still outperforms Baseline in every configuration.

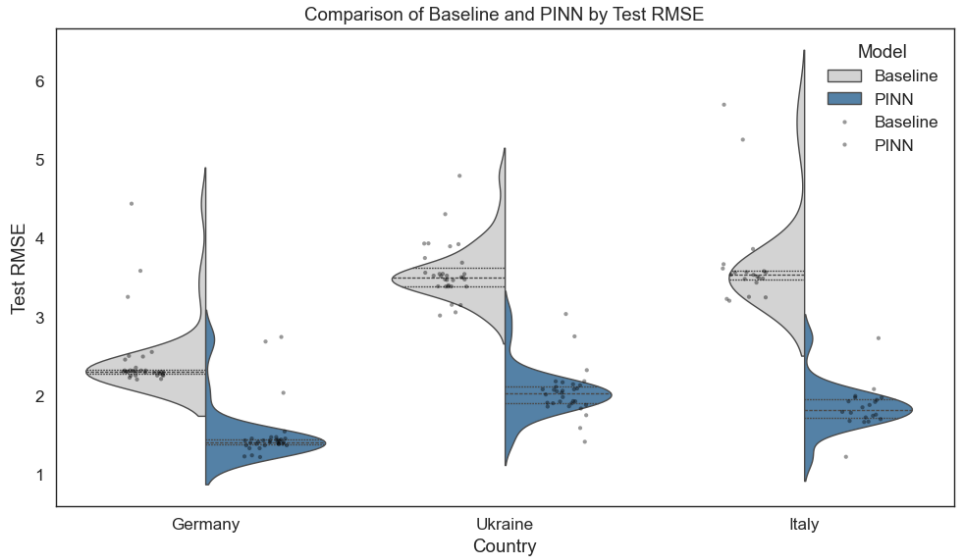

Fig. 3.1. Distribution of test RMSE for Baseline and PINN across three countries

To confirm these findings, Figure 3.2 presents a pairwise comparison of the test RMSE for PINN and Baseline in each configuration. Each point corresponds to a distinct combination of model parameters, and the diagonal line $(y = x)$ indicates equality of errors. All points lie below this line, confirming PINN's consistent advantage over Baseline. The color coding shows that the largest gain is observed in Italy, and the smallest in Germany, which is consistent with the results in Figure 3.1.

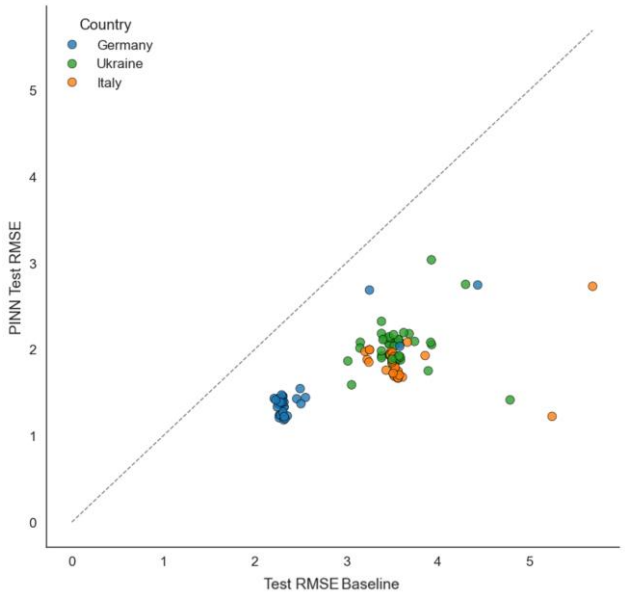

Fig. 3.2. Paired comparison of test *RMSE* for PINN and Baseline

A summary of the results is presented in Table 3.1, where for each country and value of the parameter k (number of covariates), the mean values *of RMSE* and the coefficient of determination R^2 are given

ISSN 3083-7715 (online) Автоматизовані системи управління та прилади автоматики. 2026. № 2 (189)
ISSN 3083-7650 (0135-1710) (print) Management Information System and Devices. 2026. No. 2 (189)

for both models. It can be seen that regardless of the number of covariates, PINN demonstrates lower *RMSE* and higher R^2, confirming its ability to better align with the data.

Statistical analysis confirmed that PINN models yield significantly lower test *RMSE* values compared to the baseline (paired tests with FDR correction; all key comparisons have adjusted $p < 0.01$). Experiments with models having one and eight covariates confirm that switching to PINN is associated with a reduction *in RMSE* of approximately 1.42 units from the baseline ($p < 0.001$; Table 3.2).

Table 3.1. *Comparison of the quality of the Baseline and PINN models based on test RMSE and* R^2 *for different countries and numbers of covariates* k

Country	k	Baseline RMSE	PINN RMSE	Baseline R^2	PINN R^2
Germany	0	2.35	1.42	0.87	0.95
Germany	1	2.60	1.67	0.84	0.93
Germany	8	2.61	1.59	0.85	0.94
Italy	0	3.32	1.89	0.91	0.97
Italy	1	4.24	1.92	0.85	0.97
Italy	8	3.66	1.90	0.89	0.97
Ukraine	0	3.42	2.02	0.91	0.97
Ukraine	1	3.96	2.05	0.87	0.96
Ukraine	8	3.63	2.21	0.89	0.96

Table 3.2. *Statistical analysis of RMSE comparisons in PINN and baseline models*

country	Germany		Italy		Ukraine		
k	1	8	1	1	1	1	8
window_len	21	21	14	21	14	21	21
n	16	9	9	10	9	10	5
mean_pinn	1.472	1.628	1.652	2.011	1.852	2.167	2.287
mean_base	2.371	2.684	3.732	3.671	3.680	3.624	3.659
mean_diff	–0.899	–1.056	–2.080	–1.660	–1.828	–1.457	–1.372
std_diff	0.112	0.336	0.730	0.480	0.583	0.100	0.343
test	wilcoxon	wilcoxon	wilcoxon	wilcoxon	wilcoxon	paired_t	paired_t
stat	0	0	0	0	0	–46.187	–8.946
pval	0.00043	0.003906	0.00391	0.001953	0.0039	5.23E-12	0.00086
cohens_d_paired	–8.02671	–3.145	–2.848	–3.460	–3.133	–14.606	–4.001
ci_diff_lo	–0.94861	–1.300	–2.572	–1.973	–2.228	–1.520	–1.632
ci_diff_hi	–0.84362	–0.869	–1.821	–1.451	–1.605	–1.402	–1.091
shapiro_p	0.00143	0.009	1.03E-06	0.00012	4.21E-06	0.802	0.922
pval_adj	0.00115	0.0039	0.00391	0.00313	0.00391	4.19E-11	0.0017
reject_fdr	True	True	True	True	True	True	True

The results demonstrate that PINN not only reduces the test error but does so consistently across all countries and all model configurations. This provides a basis for further analysis of which specific factors – window length, hyperparameters, covariates, etc. – influence the magnitude of the gain, and whether the model can be further improved through the use of information variables.

3.2. The Effect of Sliding Window Length and the Stride Parameter

One of the key structural decisions in constructing the PINN model is the choice of the sliding window length (L), on which local model training is performed. The window defines the time interval during which the model parameters (specifically $\beta(t), \gamma(t)$) are considered constant or slowly changing. On the one hand, a short window allows the model to quickly adapt to local changes in epidemic dynamics; on the other hand, it can lead to instability in estimates due to an insufficient number of data points. A long window, conversely, provides smoothing but may lose sensitivity to short-term changes.

This study examines two window lengths: $L = 14$ and $L = 21$ days. This choice represents a compromise between practical constraints and epidemiological soundness. The 14-day window corresponds to the typical incubation period for COVID-19 and is widely used in statistical reports and quarantine policy. The 21-day value allows us to assess whether a longer window provides additional stability or smoothing. Other values were not systematically considered, as increasing L beyond 21 days leads to a loss of local sensitivity, while decreasing it below 14 days leads to excessive data

Автоматизовані системи управління та прилади автоматики. 2026. № 2 (189) *ISSN 3083-7715 (online)*
Management Information System and Devices. 2026. No. 2 (189) *ISSN 3083-7650 (0135-1710) (print)*

fragmentation and optimization instability. Furthermore, the limit on the number of windows in each wave does not allow for a full-scale test of shorter intervals without losing statistical power. We investigated how the choice of window length $L=14$ or $L=21$ days affects model quality, as well as how the result changes when varying the window stride parameter s (stride), which determines the frequency of window updates along the time series.

For $L=14$, *the* average test *RMSE* drops to 1.72. And for $L=21$, it rises to 1.94, and the model no longer captures rapid wave changes as well. The corresponding R-squared values are $R^2=0.965$ and $R^2=0.952$. The difference is statistically significant (Wilcoxon test, $p \ll 0.01$) and practically important, especially for waves with rapid phase transitions. This is consistent with the hypothesis that a shorter window better captures the local features of the curve, specifically the peak asymmetry, the rate of rise, and the decay.

Fig. 3.3 shows a comparison of the *RMSE* distributions for the PINN model using $L=14$ and $L=21$ days. It can be seen that the short window not only yields lower median values but also reduces the spread, indicating higher model stability.

Fig. 3.3. Distribution of test *RMSE* for PINN with different window lengths

The effect of the stride parameter (s), which determines how often the window moves along the time series, was investigated separately. The default value of $s=7$ corresponds to a weekly update, and $s=3$ and $s=10$ were additionally considered. Changing from 7 to 3 or 10 alters *the RMSE* by only ±0.05, and R^2 remains stable. This indicates that the model is robust to the choice of window update frequency, and the parameter s can be adapted to computational constraints without losing accuracy.

In summary, it can be stated that the choice of sliding window length is a critical factor for model quality. A short window $L=14$ ensures better adaptation to local dynamics, reduces overfitting, and improves the model's alignment with the data. The *stride* parameter has a secondary effect and can vary depending on computational resources. These results confirm that the structural organization of training intervals is a key element in constructing effective PINN models for epidemic time series.

3.3. The Impact of Covariates on Model Quality

The objective of this section is to quantitatively assess the role of informational covariates in explaining the difference in model quality, defined as the Δ (3.1). Positive values of Δ indicate an advantage for PINN. For a systematic analysis, we applied the following sequence of methods:

1) a basic linear model with control variables;

2) an extended model with indicators of covariate presence and an assessment of their combined contribution via partial- R^2;

3) dimensionality reduction of the covariate block using principal component analysis (PCA);

4) a regularized Lasso model as a stability check.

ISSN 3083-7715 (online) *Автоматизовані системи управління та прилади автоматики. 2026. № 2 (189)*
ISSN 3083-7650 (0135-1710) (print) *Management Information System and Devices. 2026. No. 2 (189)*

This structure allows to separate the influence of structural parameters and cross-country differences from the contribution of informational covariates.

The main analysis was performed for three values *of* k : a model without covariates $(k=0)$, a model with one covariate $(k=1)$, and a model with the full set of eight variables $(k=8)$. It is important to emphasize that the case $(k=1)$ is not a single model: eight separate models were constructed, each containing only one of the eight available covariates. This allows us to assess the individual contribution of each variable without the influence of multicollinearity and to identify the potentially most informative one.

In addition, for each country, an additional series of "cumulative" models was built, in which covariates were added gradually: first two, then three, and so on up to eight. These models used a standard set of other parameters (window length, stride, α), allowing us to assess whether model quality improves as the information space increases, or whether adding new variables leads to overfitting and a decline in fit.

Fig. 3.4 shows the distribution of test *RMSE* values for PINN models with different numbers of covariates k. Fig. 3.5 shows the distribution of test *RMSE* values for PINN models for each of the eight covariates individually.

Changes in the median and density of the distributions help to visually assess the impact of additional covariates on forecast quality.

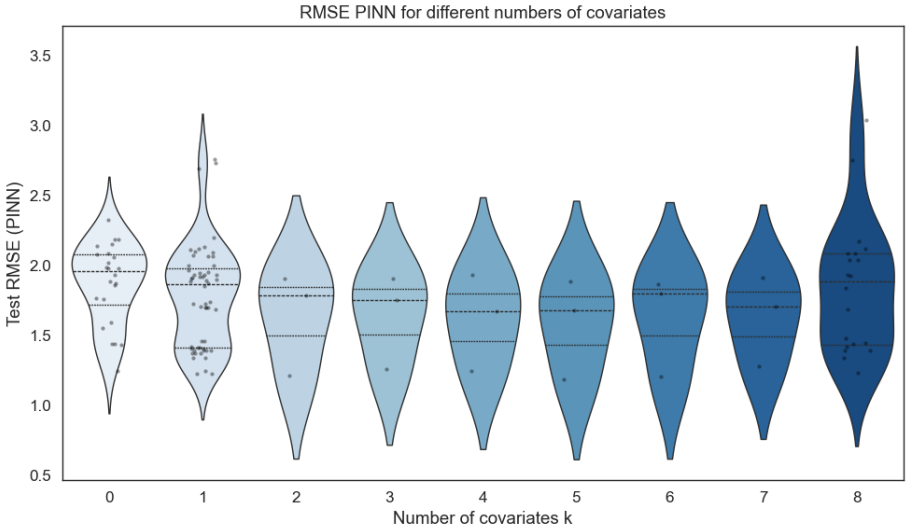

Fig. 3.4. Distribution of PINN test *RMSE* by number of covariates

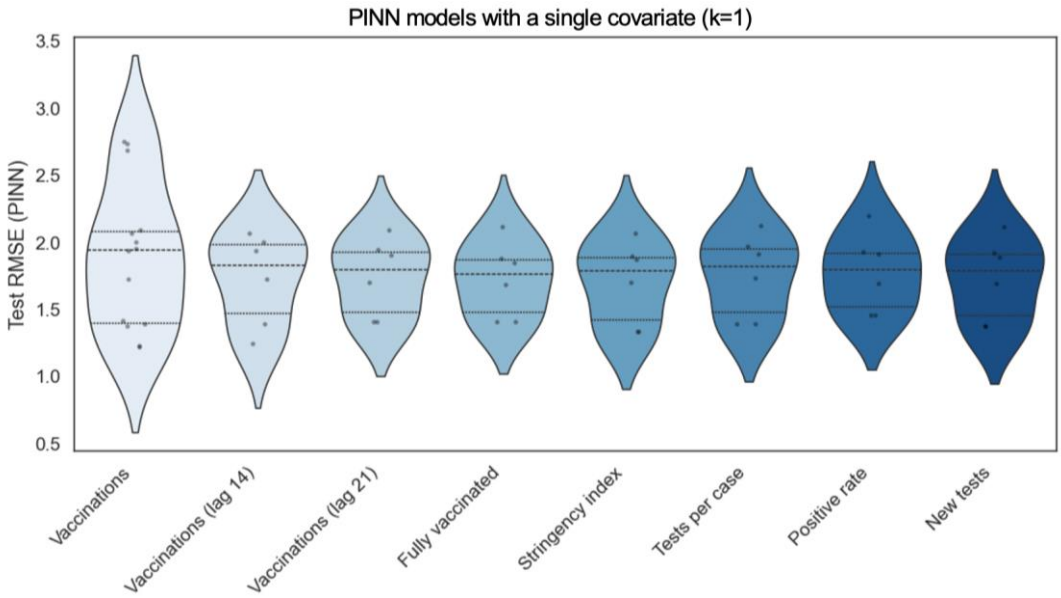

Fig. 3.5. Test RMSE of PINN for models with a single covariate

Автоматизовані системи управління та прилади автоматики. 2026. № 2 (189) *ISSN 3083-7715 (online)*
Management Information System and Devices. 2026. No. 2 (189) *ISSN 3083-7650 (0135-1710) (print)*

Covariates have a weak and often varying effect in each country. In Germany, adding variables often leads to a slight deterioration *in RMSE*, which may be due to the high quality of the baseline data and the relatively smooth waveform, which PINN reproduces well even without additional factors. In Italy and Ukraine, the picture is mixed: some individual covariates (primarily vaccination indicators) sometimes yield a slight improvement, but in other configurations the effect disappears or changes sign.

Baseline linear model

The initial baseline estimation was performed using a linear model:

$$\Delta_i = \beta_0 + \gamma_{\text{Italy}} \cdot 1\{\text{Italy}_i\} + \gamma_{\text{Ukraine}} \cdot 1\{\text{Ukraine}_i\} + \beta_L \cdot \text{window\_len}_i + \beta_\alpha \cdot \alpha_i + \beta_s \cdot stride_i + \varepsilon_i \quad (3.2)$$

where ε_i is the random error. Parameter estimation was performed using the least squares method: $\hat{\beta} = \left(X^{\mathrm{T}} X\right)^{-1} X^{\mathrm{T}} y$.

Due to possible heteroscedasticity of the residuals (Table 3.3), we used robust standard errors of the HC3 type [25, 33]. All standard errors and confidence intervals presented in the tables are adjusted specifically for HC3.

The results of the baseline model are presented in Table 3.4. Country effects and the window_len parameter remain significant, with the latter having a consistently negative effect on the Δ, i.e., longer windows reduce the PINN gain.

Table 3.3. *Statistics on the normality of residuals and identification of potential outliers*

Metric	Value
Omnibus	122.684
Prob(Omnibus)	0.000
Jarque–Bera	1840.597
Skew	3.641
Kurtosis	20.926
Max leverage	0.1517
Number of observations with |std_resid| > 3	several

Table 3.4. *Results of the baseline OLS model with HC3 correction*

Parameter	Estimate	SE (HC3)	*t*	*p* **-value**
Intercept	0.8820	0.736	1.198	0.231
C(country)[Italy]	0.7272	0.088	8.240	0.000
C(country)[Ukraine]	0.5038	0.056	9.072	0.000
window_len	–0.0367	0.009	–3.952	0.000
α	0.1666	0.793	0.210	0.834
stride	0.0936	0.031	2.996	0.003

Based on our data, the covariate block yields $R^2_{\text{partial}} \approx 0.154$, and the 95% bootstrap confidence interval for the partial R^2 is [0.054, 0.342] [34]. This means that the covariates make a moderate but not dominant contribution to explaining Δ. The coefficients of the regression model are presented in Table 3.5.

Table 3.5. *Regression coefficients of the full model with indicators (HC3)*

Parameter	Estimate	SE (HC3)	*t*	*p* – value
Intercept	0.9518	0.738	1.290	0.197
C(country)[Italy]	0.7135	0.080	8.903	0.000
C(country)[Ukraine]	0.5134	0.059	8.716	0.000
$window\_len$	–0.0452	0.012	–3.712	0.000
α	0.1753	0.738	0.237	0.812
stride	0.0902	0.048	1.891	0.059
Vaccinations	0.3933	0.210	1.869	0.062
Vaccinations (lag 14)	–0.3730	0.175	–2.127	0.033
Fully vaccinated	0.1209	0.050	2.395	0.017
Stringency index	0.1061	0.039	2,753	0.006

ISSN 3083-7715 (online) Автоматизовані системи управління та прилади автоматики. 2026. № 2 (189)
ISSN 3083-7650 (0135-1710) (print) Management Information System and Devices. 2026. No. 2 (189)

PCA of the covariate block

To reduce multicollinearity in the covariate block, we applied the principal component analysis (PCA) method and used the first two components (PC1 and PC2), which explain ≈76% of the variance [35]. This allowed us to stabilize the estimates without losing information.

The first component, PC1, explains ≈62% of the block's variance and has positive loadings (approximately 0.28–0.39) on all indicators, allowing it to be interpreted as an aggregated index of covariate presence. The second principal component, PC2 (≈14%), reflects the contrast between types of covariates (e.g., vaccination and testing indicators). Using PC1/PC2 as predictors in the regression reduces VIF and stabilizes the estimates of structural parameters.

Lasso Regularized Model

To test the robustness of the results, we applied the **Lasso** regularized model. The objective function is written as:

$$\hat{\beta}_{\text{lasso}} = \arg\min_{\beta} \left\{ \sum_i (y_i - X_i\beta)^2 + \lambda_{\text{lasso}} |\beta|_1 \right\}. \quad (3.3)$$

Lasso selected a very small λ_{lasso} and set almost all indicators to zero, leaving only window_len as a stable predictor (Table 3.6). This confirms that structural parameters have a greater and more stable influence on Δ than individual informational covariates.

Table 3.6. *Results of regularized estimates: optimal parameters and stable coefficients*

Method	Best value of the regularization hyperparameter	Key coefficients
LassoCV	$\lambda_{\text{lasso}} = 0.0340$	$window\_len = -0.1608$; $\alpha = 0.0000$; $stride = 0.0244$

Diagnosis of residuals and multicollinearity

Diagnosis of residuals and influential observations was performed using standard statistics: Omnibus, Jarque-Bera (JB), skewness and kurtosis coefficients, as well as leverage and standardized residuals (std_resid).

In the experiments, Omnibus and JB had very small p-values, skewness ≈ 2.5–3.7, and kurtosis ≈ 15–21, indicating strong skewness and heavy tails in the residual distribution. There are also several observations with high residual standard deviations ( ) – potential outliers with $(|std\_resid| > 3)$. Therefore, we applied HC3 and conducted a sensitivity analysis: we repeated the OLS (HC3) without the observations – potential outliers with $(|std\_resid| > 3)$. As a result, the changes in the main coefficients and partial-R^2 s were insignificant; thus, the conclusions are considered robust to the influence of individual outliers.

Fig. 3.6 shows the dependence of leverage on standardized residuals for the full model with indicators (HC3 estimates) and allows for the visual identification of potentially influential observations (points with $|std\_resid| > 3$) and increased leverage.

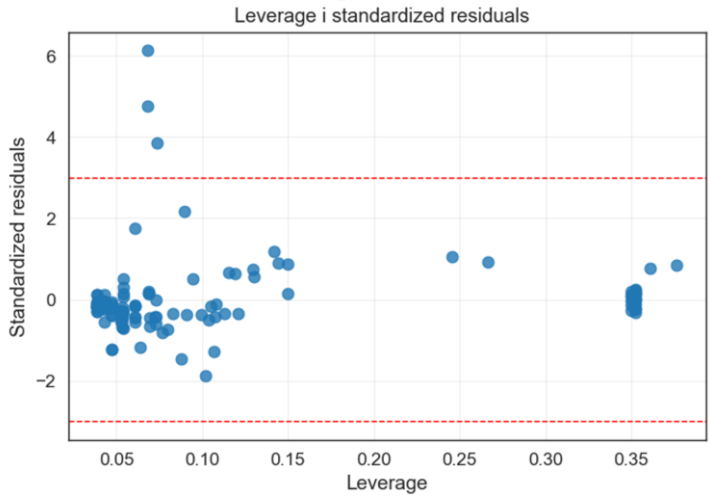

Fig. 3.6. Leverage and standardized residuals – diagnosis of influential observations

Автоматизовані системи управління та прилади автоматики. 2026. № 2 (189) *ISSN 3083-7715 (online)*
Management Information System and Devices. 2026. No. 2 (189) *ISSN 3083-7650 (0135-1710) (print)*

To diagnose multicollinearity, we used the variance inflation factor (VIF), which is defined as

$$\mathrm{VIF}_j = \frac{1}{1-R_j^2}, \qquad (3.4)$$

where R_j^2 is the coefficient of determination for the regression of X_j on other predictors.

VIF (Table 3.7) does not exceed ≈3.6, indicating the absence of serious multicollinearity.

Table 3.7. *VIF analysis of multicollinearity after adjustments*

Variable	VIF
Vaccinations (week 21)	3.5703
Vaccinations (14-day lag)	3.5638
Fully vaccinated	2.9364
Stringency index	2.7500
Vaccinations	2.5938
Tests per case	2.5814
Positive rate	2.3759
New tests	2.0448
window_len	1.2885
α	1.0325
stride	1.0010

4. Conclusion

Thus, statistical tests provide a consistent picture: **PINN almost always outperforms Baseline**; structural parameters, primarily sliding window length and inter-region differences, are the main factors behind the difference in model quality and PINN's advantage. The block of information covariates has a moderate partial contribution $\left(R^2 \approx 0.154\right)$, but individual covariates provide a weak and unstable signal. PCA and Lasso consistently confirm these conclusions.

These results are consistent with the assumption that the local form of the epidemic wave (the FSIR-PINN window structure) already contains integrated information about external influences through the shape of the epidemic wave, specifically vaccination, changes in mobility, and behavioral factors. PINN reproduces these effects by adapting the parameters $\beta(t)$ and $\gamma(t)$ within each sliding window. Noise and multicollinearity negate the potential informational contribution of covariates; therefore, their explicit inclusion does not provide a significant improvement in model quality.

Further research should focus on extending the PINN sensitivity analysis to other infectious diseases and epidemic waves with different dynamics. A promising direction is the development of adaptive methods for automatically selecting the sliding window length based on local dynamics characteristics. It is also worth investigating alternative approaches to integrating covariates, particularly through attention mechanisms, which can mitigate the negative impact of multicollinearity. Furthermore, it is advisable to apply PINN in multi-population models that account for spatial interactions between regions, as well as to compare it with other classes of physically informed architectures, such as DeepONet and the Fourier Neural Operator.

Conflict of Interest

The authors confirm that the study was conducted in the absence of any commercial or financial relationships that could be construed as a potential conflict of interest.

Funding

The study was conducted without financial support.

Data Availability

The manuscript contains data in the form of electronic supplementary material.

Use of Artificial Intelligence

The author confirms that no AI technologies were used in the preparation of this work.

References

1. Kermack, W. O., McKendrick, A. G. (1927), "A contribution to the mathematical theory of epidemics", *Proceedings of the Royal Society*, Vol. 115, pp. 700–721. DOI: https://doi.org/10.1098/rspa.1927.0118
2. Kalachev, L., et al. (2023), "Revisiting classical SIR modelling in light of the COVID-19 pandemic", *Infectious Disease Modelling*, Vol. 8, No. 3, pp. 72–83. DOI: https://doi.org/10.1016/j.idm.2022.12.002
3. Nesteruk, I. (2020), "Simulations and Predictions of COVID-19 Pandemic With the SIR Model", *Innovative Biosystems and Bioengineering*, Vol. 4(1), pp. 20–29. DOI: https://doi.org/10.20535/ibb.2020.4.2.204274

ISSN 3083-7715 (online) *Автоматизовані системи управління та прилади автоматики. 2026. № 2 (189)*
ISSN 3083-7650 (0135-1710) (print) *Management Information System and Devices. 2026. No. 2 (189)*

4. Mohajan, H. (2022), "Mathematical Analysis of SIR Model for COVID-19 Pandemic", *MPRA Paper*, No. 114390. DOI: https://mpra.ub.uni-muenchen.de/114390/
5. Voronin, A., Akhiiezer, O., Galuza, A., Lebedeva, I., Zaitsev, Yu., Lebedev, S. (2023), "Modeling Competitive Interaction «Predator-Prey» on the Example of Two Innovative Processes", *13th International Conference on Advanced Computer Information Technologies (ACIT), Wrocław, Poland*. pp. 131–134. DOI: https://doi.org/10.1109/ACIT58437.2023.10275538
6. Raissi, M., Perdikaris, P., Karniadakis, G. E. (2019), "Physics-informed neural networks: A deep learning framework for solving forward and inverse problems involving nonlinear partial differential equations", *Journal of Computational Physics*, Vol. 378, pp. 686–707. DOI: https://doi.org/10.1016/j.jcp.2018.10.045
7. Raissi, M., Perdikaris, P., Karniadakis, G.E. (2017), "Physics Informed Deep Learning (Part II): Data-driven Discovery of Nonlinear Partial Differential Equations", *Artificial Intelligence*, DOI: https://doi.org/10.48550/arXiv.1711.10566
8. Lyubchyk, L., Grinberg, G., Lyubchyk, M., Galuza, A., Akhiiezer, O. (2020), "Interval Evaluation of Stationary State Probabilities for Markov Set-Chain Models", *10th IEEE International Conference on Advanced Computer Information Technologies (ACIT), Deggendorf, Germany*, pp. 82–85. DOI: https://doi.org/10.1109/ACIT49673.2020.9208932
9. Kozioł, K., Latosińska, J. N., Kozioł, M. (2020), "Fractional-Order SIR Epidemic Model for Transmission of COVID-19", *Applied Sciences*, Vol. 10(23), pp. 8316. DOI: https://doi.org/10.3390/app10238316
10. Banerjee, R., Bhattacharyya, R., Roy, T. K. (2022), "Fractional optimal control of compartmental SIR model for COVID-19 with Caputo's fractional derivative", *IFAC-PapersOnLine*, Vol. 55(2), pp. 349–354. DOI: https://doi.org/10.1016/j.ifacol.2022.04.101
11. Alshomrani, A. S., Khan, A., Ahmad, I., Baleanu, D. (2021), "Caputo SIR model for COVID-19 under optimized fractional order", *Chaos, Solitons & Fractals.* Vol. 143, pp. 110619. DOI: https://doi.org/10.1186/s13662-021-03345-5
12. Cuomo, S., Di Cola, V. S., Giampaolo, F., Rozza, G., Raissi, M., Piccialli, F. (2022), "Scientific Machine Learning Through Physics-Informed Neural Networks: Where we are and what's next", *Journal of Scientific Computing*, Vol. 92(3), Art. 88. DOI: https://doi.org/10.1007/s10915-022-01939-z
13. Wang, S., Yu, X., Perdikaris, P. (2022), "When and why PINNs fail to train: A neural tangent kernel perspective", *Journal of Computational Physics*, Vol. 449, Art. 110768. DOI: https://doi.org/10.1016/j.jcp.2021.110768
14. Kharazmi, E., Cai, M., Zheng, X., Zhang, Z., Lin, G., Karniadakis, G. E. (2022), "Identifiability and predictability of integer- and fractional-order epidemiological models using physics-informed neural networks", *Nature Computational Science*, Vol. 2, pp. 744-753. DOI: https://doi.org/10.1101/2021.04.05.21254919
15. McClenny, L. D., Braga-Neto, U. M. (2023), "Self-Adaptive Physics-Informed Neural Networks", *Journal of Computational Physics*, Vol. 474, Art. 111722. DOI: https://doi.org/10.1016/j.jcp.2022.111722
16. Cai, S., Mao, Z., Wang, Z., Yin, M., Karniadakis, G. E. (2021), "Physics-informed neural networks (PINNs) for fluid mechanics: A review", *Acta Mechanica Sinica*, Vol. 37, pp. 1727–1738. DOI: https://doi.org/10.1007/s10409-021-01148-1
17. Cramer, E. Y., et al. (2022), "Evaluation of individual and ensemble probabilistic forecasts of COVID-19 mortality in the United States", *Proceedings of the National Academy of Sciences*, Vol. 119(15), Art. e2113561119. DOI: https://doi.org/10.1073/pnas.2113561119
18. Mishra, S., Molinaro, R. (2022), "Estimates on the generalization error of physics-informed neural networks for approximating a class of inverse problems for PDEs", *IMA Journal of Numerical Analysis*, Vol. 42(2), pp. 981–1022. DOI: https://doi.org/10.1093/imanum/drab032
19. Our World in Data (OWID) – COVID-19 dataset (data source). IEEE DataPort entry (DOI for dataset snapshot). DOI: https://doi.org/10.21227/2n61-4965
20. Caputo, M. (1967), "Linear models of dissipation whose Q is almost frequency independent", *Geophysical Journal International*. DOI: https://doi.org/10.1111/j.1365-246X.1967.tb02303.x
21. Diethelm, K. (2010), "The Analysis of Fractional Differential Equations", *Springer.* DOI: https://doi.org/10.1007/978-3-642-14574-2
22. Danane, J, Hammouch, Z, Allali, K, Rashid, S, Singh, J. (2021), "A fractional-order model of coronavirus disease 2019 (COVID-19) with governmental action and individual reaction", *Math Methods Appl Sci.* DOI: https://doi.org/10.1002/mma.7759
23. Kingma, D. P., Ba, J. (2013), "A method for stochastic optimization", *ICLR (arXiv).* DOI: https://doi.org/10.48550/arXiv.1412.6980
24. Benjamini, Y., Hochberg, Y. (1995), "Controlling the false discovery rate: A practical and powerful approach to multiple testing", *JRSS.* DOI: https://doi.org/10.1111/j.2517-6161.1995.tb02031.x
25. MacKinnon, J. G., White, H. (1985), "Some heteroscedasticity – consistent covariance matrix estimators with improved finite sample properties", *Journal of Econometrics*. DOI: https://doi.org/10.1016/0304-4076(85)90158-7
26. White, H. (1980), "A heteroscedasticity – consistent covariance matrix estimator and a direct test for heteroskedasticity", *Econometrica*. DOI: https://doi.org/10.2307/1912934
27. Bates, D., Mächler, M., Bolker, B., Walker, S. (2015), "Fitting linear mixed – effects models using lme", *Journal of Statistical Software*, Vol. 67, Issue 1. DOI: https://doi.org/10.18637/jss.v067.i01
28. O'Brien, R. M. (2007), "A Caution Regarding Rules of Thumb for Variance Inflation Factors", *Quality & Quantity.* DOI: https://doi.org/10.1007/s11135-006-9018-6
29. *Applied Regression Analysis and Generalized Linear Models* (3rd ed.). John Fox, Sage.

30. James, G. et al. (2023), "An Introduction to Statistical Learning (2nd ed.)", *Springer*.
31. Pedregosa, F. et al. (2011), "Scikit – learn: Machine learning in Python", *JMLR*. DOI: https://doi.org/10.48550/arXiv.1201.0490
32. Hastie, T., Tibshirani, R., Friedman, J. (2009), "The Elements of Statistical Learning", *Springer*. DOI: https://doi.org/10.1007/978-0-387-84858-7
33. Long, J. S., Ervin, L. H. (2000), "Using heteroscedasticity consistent standard errors in the linear regression model", *The American Statistician*, Vol. 54, No. 3. pp. 217–224.
34. Efron B. (1979), "Bootstrap methods: Another look at the jackknife", *Ann. Statist*, Vol. 7, No. 1, pp. 1–26. DOI: https://doi.org/10.1214/aos/1176344552
35. Jolliffe, I. T., Cadima, J. (2016), "Principal component analysis: a review and recent developments", *Philosophical Transactions of the Royal Society*, No. 374(2065), pp. 20150202

Received (Надійшла) 27.02.2026
Accepted for publication (Прийнята до друку) 01.04.2026
Publication date (Дата публікації) 29.05.2026

Відомості про авторів / About the Authors

Погорєлов Станіслав Вікторович – доктор фізико-математичних наук, професор, Національний технічний університет "Харківський політехнічний інститут", професор кафедри комп'ютерної математики і аналізу даних, Харків, Україна;
Stanislav Pohorielov – Doctor of physical and mathematical sciences, Professor, National Technical University "Kharkiv polytechnic institute", Professor at the Department of Computer Mathematics and Data Analysis, Kharkiv, Ukraine;
e-mail: Stanislav.Pohorielov@khpi.edu.ua
ORCID ID: https://orcid.org/0000-0002-0189-8655

Балаба Ярослав Андрійович – Національний технічний університет "Харківський політехнічний інститут", аспірант кафедри комп'ютерної математики і аналізу даних, Харків, Україна;
Yaroslav Balaba – National Technical University "Kharkiv polytechnic institute", Postgraduate Student at the Department of Computer Mathematics and Data Analysis, Kharkiv, Ukraine;
e-mail: Yaroslav.Balaba@cs.khpi.edu.ua
ORCID ID: https://orcid.org/0009-0005-9710-2971

Татар'янц Максим Сергійович – Національний технічний університет "Харківський політехнічний інститут", старший викладач кафедри комп'ютерної математики і аналізу даних, Харків, Україна;
Maksym Tatariaiants – National Technical University "Kharkiv polytechnic institute", Senior Lecturer at the Department of Computer Mathematics and Data Analysis, Kharkiv, Ukraine;
e-mail: Maksym.Tatariants@cs.khpi.edu.ua
ORCID ID: https://orcid.org/0000-0002-5952-9801

Беркунський Євген Юрійович – Національний університет кораблебудування імені адмірала Макарова, старший викладач кафедри інформаційних управляючих систем та технологій, Миколаїв, Україна;
Yevhen Berkunskyi – Admiral Makarov National University of Shipbuilding, Senior Lecturer at the Department of Information Control Systems and Technology, Mykolaivof, Ukraine;
e-mail: yevgen.berkunskyy@nuos.edu.ua
ORCID ID: https://orcid.org/0000-0001-8876-1784

Павленко Альона Юріївна – Національний університет кораблебудування імені адмірала Макарова, старший викладач кафедри інформаційних управляючих систем та технологій, Миколаїв, Україна;
Alona Pavlenko – Admiral Makarov National University of Shipbuilding, Senior Lecturer at the Department of Information Control Systems and Technology, Mykolaivof, Ukraine;
e-mail: aliona.pavlenko@nuos.edu.ua
ORCID ID: https://orcid.org/0000-0002-3776-8377

ISSN 3083-7715 (online) *Автоматизовані системи управління та прилади автоматики. 2026. № 2 (189)*
ISSN 3083-7650 (0135-1710) (print) *Management Information System and Devices. 2026. No. 2 (189)*

СИСТЕМАТИЧНИЙ АНАЛІЗ ЧУТЛИВОСТІ ФІЗИЧНО-ІНФОРМОВАНИХ НЕЙРОННИХ МЕРЕЖ У ЗАДАЧАХ МОДЕЛЮВАННЯ ЕПІДЕМІЧНИХ ЧАСОВИХ РЯДІВ

У статті подано систематичний аналіз чутливості фізично-інформованих нейронних мереж (PINN) у задачах моделювання епідемічних часових рядів. **Мета дослідження** – проведення систематичного аналізу чутливості PINN-моделей на реальних епідемічних часових рядах і визначення ключових факторів, що впливають на якість відтворення динаміки епідемічних хвиль. **Завдання:** оцінити вплив довжини ковзного вікна, набору коваріат, параметрів регуляризації та випадкової ініціалізації на якість PINN; порівняти PINN із класичною *baseline*-моделлю без фізичних обмежень. **Методи:** масштабна серія експериментів для трьох країн із варіюванням довжини ковзного вікна, кроку зсуву, порядку дробової похідної α, стохастичної стабільності та набору коваріат; статистичний аналіз із застосуванням тесту Вілкоксона, OLS із HC3-корекцією, PCA та *Lasso*-регуляризації. **Результати:** PINN майже завжди дає кращі метрики, ніж *baseline*, за точністю відтворення епідемічних часових рядів і демонструє вищі значення R^2 та нижчі RMSE/MAE у всіх країнах. Установлено, що 14-денне ковзне вікно забезпечує оптимальний баланс між адаптивністю та стійкістю моделі, тоді як збільшення довжини ковзного вікна до 21 дня призводить до згладжування динаміки та втрати локальної чутливості. Проведені експерименти продемонстрували, що ефект коваріат не має універсального позитивного результату. У деяких конфігураціях додаткові змінні в певних країнах покращують якість моделі, тоді як в інших додають шуму через мультиколінеарність і низьку якість даних. Дослідження стабільності підтвердило низьку чутливість PINN до випадкової ініціалізації та параметрів регуляризації. Досягнуті результати дають змогу чітко побачити поведінку PINN-моделей у задачах епідеміологічного моделювання та визначають практичні рекомендації щодо вибору параметрів, які забезпечують надійність і відтворюваність моделі. **Висновки:** PINN є більш ефективною альтернативою класичним моделям для епідемічного моделювання; 14-денне ковзне вікно є оптимальним; вплив коваріат не стабільний і залежить від країни.

Ключові слова: фізично-інформовані нейронні мережі (PINN); епідемічні часові ряди; аналіз чутливості; ковзне вікно; коваріати; стабільність моделі; машинне навчання; нейронні мережі; епідеміологічне моделювання.

Бібліографічні описи / Bibliographic descriptions

Погорєлов С. В., Балаба Я. А., Татар'янц М. С., Беркунський Є. Ю., Павленко А. Ю. Систематичний аналіз чутливості фізично-інформованих нейронних мереж у задачах моделювання епідемічних часових рядів. *Автоматизовані системи управління та прилади автоматики*. 2026. № 2 (189). С. 309–324. DOI: https://doi.org/10.30837/0135-1710.2026.189.309

Pohorielov, S., Balaba, Y., Tatariaiants, M., Berkunskyi, Y., Pavlenko, A. (2026), "A systematic sensitivity study of physics-informed neural networks for epidemic time series", *Management Information System and Devices*, No. 2 (189), P. 309–324. DOI: https://doi.org/10.30837/0135-1710.2026.189.309